

The clustering of galaxies in the completed SDSS-III Baryon Oscillation Spectroscopic Survey: a tomographic analysis of structure growth and expansion rate from anisotropic galaxy clustering

Yuting Wang^{1,2*}, Gong-Bo Zhao^{1,2†}, Chia-Hsun Chuang³, Marcos Pellejero-Ibanez^{4,5},
Cheng Zhao^{6,1}, Francisco-Shu Kitaura³, Sergio Rodriguez-Torres^{7,8}

¹ National Astronomy Observatories, Chinese Academy of Science, Beijing, 100012, P. R. China

² Institute of Cosmology & Gravitation, University of Portsmouth, Dennis Sciamia Building, Portsmouth, PO1 3FX, UK

³ Leibniz-Institut für Astrophysik Potsdam (AIP), An der Sternwarte 16, D-14482 Potsdam, Germany

⁴ Instituto de Astrofísica de Canarias (IAC), C/Vía Láctea, s/n, E-38200, La Laguna, Tenerife, Spain

⁵ Departamento Astrofísica, Universidad de La Laguna (ULL), E-38206 La Laguna, Tenerife, Spain

⁶ Tsinghua Center of Astrophysics and Department of Physics, Tsinghua University, Beijing 100084, China

⁷ Campus of International Excellence UAM+CSIC, Cantoblanco, E-28049 Madrid, Spain

⁸ Departamento de Física Teórica, Universidad Autónoma de Madrid, Cantoblanco, E-28049, Madrid, Spain

9 February 2022

ABSTRACT

We perform a tomographic analysis of structure growth and expansion rate from the anisotropic galaxy clustering of the combined sample of Baryon Oscillation Spectroscopic Survey (BOSS) Data Release 12, which covers the redshift range of $0.2 < z < 0.75$. In order to extract the redshift information of anisotropic galaxy clustering, we analyse this data set in nine overlapping redshift slices in configuration space and perform the joint constraints on the parameters $\{D_V \times (r_d^{\text{fid}}/r_d), F_{\text{AP}}, f\sigma_8\}$ using the correlation function multipoles. The analysis pipeline is validated using the MultiDark-Patchy mock catalogues. We obtain a measurement precision of 1.5%–2.9% for $D_V \times (r_d^{\text{fid}}/r_d)$, 5.2%–9% for F_{AP} and 13.3%–24% for $f\sigma_8$, depending on the effective redshift of the slices. We report a joint measurement of $\{D_V \times (r_d^{\text{fid}}/r_d), F_{\text{AP}}, f\sigma_8\}$ with the full covariance matrix in nine redshift slices. We use our joint BAO and RSD measurement combined with external datasets to constrain the gravitational growth index γ , and find $\gamma = 0.656 \pm 0.057$, which is consistent with the Λ CDM prediction within 95% CL.

Key words:

large scale structure of Universe; redshift space distortions; baryon acoustic oscillations

1 INTRODUCTION

The galaxy redshift survey is a powerful probe for the nature of dark energy (DE) and gravity, both of which are crucial to understanding the accelerating expansion of the Universe at late times, as discovered by observations of type Ia supernovae (Riess et al. 1998; Perlmutter et al. 1999). Redshift surveys allow us to measure the cosmic expansion history and structure growth simultaneously by statistically analysing the three-dimensional clustering of the galaxies in terms of the correlation function in configuration space or the

power spectrum in Fourier space (Cole et al. 1995; Peacock et al. 2001; Cole et al. 2005; Hawkins et al. 2003; Eisenstein et al. 2005; Okumura et al. 2008; Percival & White 2009).

The observed baryon acoustic oscillations (BAO), as a “standard ruler”, in the correlation function or power spectrum can be used to probe the cosmic expansion history, since the signal is robust to systematic uncertainties (Eisenstein & White 2004; Padmanabhan & White 2009; Mehta et al. 2011; Vargas-Magaña et al. 2016). The measured BAO scales in the radial and transverse directions from the anisotropic galaxy clustering provide an estimate of the Hubble parameter, $H(z)$, and angular diameter distance, $D_A(z)$, respectively.

The anisotropy in the galaxy clustering is partially due to the

* Email: ytwang@nao.cas.cn

† Email: gbzhao@nao.cas.cn

Alcock-Paczynski (AP) effect (Alcock & Paczynski 1979), which arises from assuming a wrong cosmology to convert redshifts to distances for the clustering analysis. The distortion of distances along and perpendicular to the line-of-sight (LOS) direction depends on the offset in the Hubble parameter, $H(z)$ and the angular diameter distance, $D_A(z)$ respectively. Therefore, measuring the relative distortion in the radial and transverse directions provides a probe of $D_A(z)$ and $H(z)$. Another source of anisotropy in galaxy clustering arises from the large-scale redshift-space distortions (RSD) (Kaiser 1987), which is the consequence of peculiar motions of galaxies. Galaxies tend to infall towards the local over-density region, thus the clustering along the LOS is enhanced. The measurement of RSD can provide us with the growth history of large-scale structure, which is parametrized as $f(z)\sigma_8(z)$, here $f(z)$ is the growth rate, and $\sigma_8(z)$ is the linear-theory root mean square (rms) mass fluctuations in spheres of radius $8 h^{-1}$ Mpc (Song & Percival 2009; Percival & White 2009), and can be used to distinguish various theoretical models, including tests of gravity (Song & Percival 2009; Raccanelli et al. 2013; Samushia et al. 2013; Beutler et al. 2014; Mueller et al. 2016).

The Baryon Oscillation Spectroscopic Survey (BOSS) (Dawson et al. 2013), part of SDSS-III (Eisenstein et al. 2011), has provided the final Data Release 12 (DR12) (Alam et al. 2015), which is the largest data set for galaxy redshift surveys to date, and includes spectroscopic redshifts of more than a million galaxies. Gil-Marín et al. (2016) carried out a RSD analysis in Fourier space using the DR12 CMASS catalogue in the redshift range of $0.43 < z < 0.75$ and the LOWZ catalogue in the redshift range of $0.15 < z < 0.43$. Using these samples, Pellejero-Ibanez et al. (2016) and Chuang et al. (2016) performed an analysis of the anisotropic clustering in configuration space. Using the “combined” sample of BOSS DR12 covering the redshift range of $0.2 < z < 0.75$ (Alam et al. 2016), a joint analysis of cosmic expansion rate and growth structure from the anisotropic clustering of galaxy was performed in (Alam et al. 2016; Beutler et al. 2017; Satpathy et al. 2017; Sánchez et al. 2017b,a; Grieb et al. 2017) in three redshift slices of $0.2 < z < 0.5$, $0.4 < z < 0.6$ and $0.5 < z < 0.75$. In order to extract the lightcone information of galaxy clustering, we performed the BAO analysis by splitting the sample into multiple overlapping redshift slices in configuration space (Wang et al. 2017) and in Fourier space (Zhao et al. 2017), respectively.

In this paper, we perform a joint BAO and RSD analysis in nine overlapping redshift slices using the correlation function multipoles from the pre-reconstructed catalogues of BOSS DR12 and the data covariance matrix estimated from the MultiDark-Patchy (MD-P) mock catalogues (Kitaura et al. 2016) (see Wang et al. (2017) for details of the correlation function measurements). We adopt the “Gaussian streaming model” (GSM) developed in (Reid & White 2011) as the template. We review GSM and the fitting method in Section 2. Our results are presented in Section 3. Section 4 is devoted to the conclusion. In this paper, we use a fiducial Λ CDM cosmology with parameters: $\Omega_m = 0.307$, $\Omega_b h^2 = 0.022$, $h = 0.6777$, $n_s = 0.96$, $\sigma_8 = 0.8288$. The comoving sound horizon in this cosmology is $r_d^{\text{fid}} = 147.74$ Mpc.

2 METHODOLOGY

2.1 Theoretical model

We use the “Gaussian streaming model” (GSM) developed in (Reid & White 2011) to compute the theoretical correlation function. The

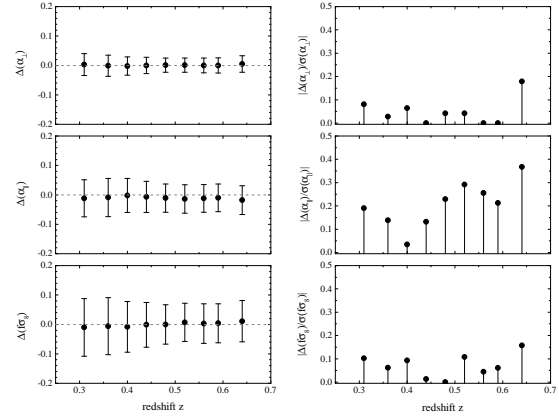


Figure 1. Left panels: The difference between the mean and the expected values. Right panels: the significance of the bias in terms of the 68% CL uncertainty.

Table 1. The mean value with 68% CL error of the anisotropic BAO parameters, α_\perp and α_\parallel and the large-scale RSD parameter, $f\sigma_8$ derived from mock catalogues. The values of $f\sigma_8$ for nine redshift slices in the fiducial cosmology are shown in the last column.

z_{eff}	α_\perp	α_\parallel	$f\sigma_8$	$(f\sigma_8)_{\text{fid}}$
0.31	1.003 ± 0.037	0.988 ± 0.063	0.469 ± 0.098	0.479
0.36	0.999 ± 0.036	0.991 ± 0.065	0.474 ± 0.097	0.48
0.40	0.998 ± 0.031	0.998 ± 0.058	0.473 ± 0.086	0.481
0.44	1.000 ± 0.028	0.993 ± 0.053	0.481 ± 0.076	0.482
0.48	1.001 ± 0.024	0.989 ± 0.048	0.482 ± 0.067	0.482
0.52	1.001 ± 0.024	0.986 ± 0.048	0.488 ± 0.065	0.481
0.56	1.000 ± 0.025	0.988 ± 0.047	0.482 ± 0.067	0.479
0.59	1.000 ± 0.026	0.990 ± 0.047	0.481 ± 0.066	0.477
0.64	1.005 ± 0.028	0.982 ± 0.049	0.486 ± 0.070	0.475

streaming model has been used to analyze the anisotropic clustering of galaxies measured from the BOSS DR9, DR11 and DR12 samples (Reid et al. 2012; Samushia et al. 2014; Pellejero-Ibanez et al. 2016; Chuang et al. 2016; Satpathy et al. 2017).

In the GSM model, the redshift-space correlation function, $\xi^s(s_\perp, s_\parallel)$ is given by (Reid & White 2011),

$$1 + \xi^s(s_\perp, s_\parallel) = \int \frac{dy}{\sqrt{2\pi} [\sigma_{12}^2(r, \mu) + \sigma_{\text{FOG}}^2]} [1 + \xi(r)] \times \exp \left\{ -\frac{[s_\parallel - y - \mu v_{12}(r)]^2}{2 [\sigma_{12}^2(r, \mu) + \sigma_{\text{FOG}}^2]} \right\}, \quad (1)$$

where $\xi(r)$ is the real-space correlation function computed using the Lagrangian perturbation theory (LPT) (Matsubara 2008). $v_{12}(r)$ is the mean infall velocity of galaxies separated by the real-space distance r , and $\sigma_{12}(r, \mu)$ is the pairwise velocity dispersion of galaxies. $v_{12}(r)$ and $\sigma_{12}(r, \mu)$ are calculated using the standard perturbation theory (SPT) (Bernardeau et al. 2002) (see Appendix A in (Reid & White 2011) for details). y is the real-space pair separation along the LOS and $\mu = y/r$. The parameter σ_{FOG}^2 accounts for the motions of galaxies (see Reid et al. (2012) for details).

A fiducial cosmology is assumed to convert the observables of

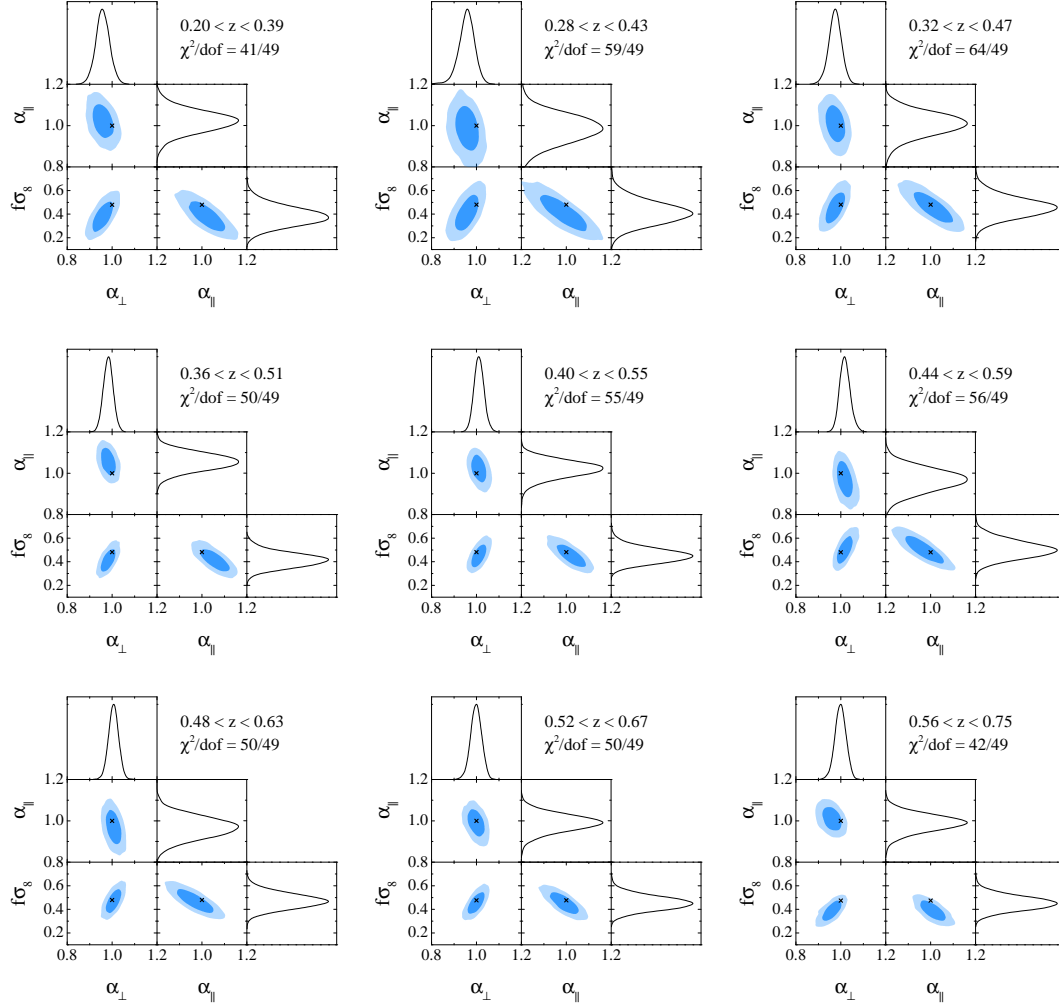


Figure 2. The measurement in nine redshift bins. We show the one-dimensional posterior distributions and the 68 and 95 % CL contour plots for parameters α_{\perp} , α_{\parallel} and $f\sigma_8$. The black cross in each panel illustrates the fiducial value.

the angular coordinates and redshifts for galaxies into distances. If the fiducial cosmology is different from the true one, it yields geometric distortions parallel and perpendicular to the LOS directions, giving rise to an anisotropy in the galaxy clustering, which is the Alcock-Paczynski (AP) effect (Alcock & Paczynski 1979). With the AP effect, the theoretical correlation function in Eq. (1) should be revised as,

$$\hat{\xi}^s(s'_{\perp}, s'_{\parallel}) = \xi^s(\alpha_{\perp}s_{\perp}, \alpha_{\parallel}s_{\parallel}), \quad (2)$$

using two scaling parameters,

$$\alpha_{\perp} = \frac{D_A(z)r_d^{\text{fid}}}{D_A^{\text{fid}}(z)r_d}, \quad \alpha_{\parallel} = \frac{H^{\text{fid}}(z)r_d^{\text{fid}}}{H(z)r_d}, \quad (3)$$

where, r_d is the sound horizon at the baryon-drag epoch. $D_A^{\text{fid}}(z)$ and $H^{\text{fid}}(z)$ are the angular diameter distance and Hubble expansion rate in the fiducial cosmology, respectively.

2.2 Parameter estimation

We compute theoretical predictions for the monopole and quadrupole correlation function using the `CosmoXi2D` code¹ (Reid & White 2011), and use a modified version of `CosmoMC`² (Lewis & Bridle 2002) for parameter estimation. We sample the parameter space of,

$$\mathbf{p} \equiv \{\alpha_{\perp}, \alpha_{\parallel}, b\sigma_8, f\sigma_8, \sigma_{\text{FOG}}^2\}, \quad (4)$$

with uniform priors of $\alpha_{\perp} \in [0.8, 1.2]$, $\alpha_{\parallel} \in [0.8, 1.2]$, $b\sigma_8 \in [1.0, 2.0]$, $f\sigma_8 \in [0.0, 1.0]$ and $\sigma_{\text{FOG}}^2 \in [0.0, 50.0] \text{ Mpc}^2$, which are conservative priors.

The χ^2 is constructed as follows,

$$\chi^2(\mathbf{p}) \equiv \sum_{i,j}^{\ell, \ell'} \left[\xi_{\ell}^{\text{th}}(s_i, \mathbf{p}) - \xi_{\ell}^{\text{obs}}(s_i) \right] F_{ij}^{\ell, \ell'} \left[\xi_{\ell'}^{\text{th}}(s_j, \mathbf{p}) - \xi_{\ell'}^{\text{obs}}(s_j) \right], \quad (5)$$

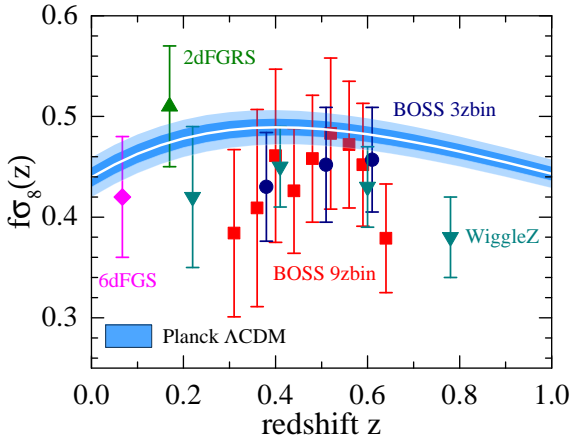
where $F_{ij}^{\ell, \ell'}$ is the inverse of the data covariance matrix estimated

¹ <http://mwhite.berkeley.edu/CosmoXi2D>

² <http://cosmologist.info/cosmomc/>

Table 2. The best-fit value with 68% CL error for parameters, α_\perp , α_\parallel and $f\sigma_8$ derived from the BOSS DR12 galaxy catalogue. We also show the derived parameters, $\{D_A \times (r_d^{\text{fid}}/r_d), H \times (r_d/r_d^{\text{fid}})\}$ or $\{D_V \times (r_d^{\text{fid}}/r_d), F_{\text{AP}}\}$.

z_{eff}	α_\perp	α_\parallel	$f\sigma_8$	$D_A \times (r_d^{\text{fid}}/r_d)$ (Mpc)	$H \times (r_d/r_d^{\text{fid}})$ ($\text{km s}^{-1} \text{Mpc}^{-1}$)	$D_V \times (r_d^{\text{fid}}/r_d)$ (Mpc)	F_{AP}
0.31	0.958 ± 0.031	1.029 ± 0.053	0.384 ± 0.083	930 ± 29	77.5 ± 4.1	1214 ± 27	0.315 ± 0.022
0.36	0.959 ± 0.035	1.012 ± 0.068	0.409 ± 0.098	1025 ± 38	81.2 ± 5.9	1376 ± 40	0.378 ± 0.034
0.40	0.972 ± 0.028	1.019 ± 0.057	0.461 ± 0.086	1113 ± 32	82.5 ± 4.9	1526 ± 34	0.430 ± 0.032
0.44	0.979 ± 0.021	1.066 ± 0.041	0.426 ± 0.062	1190 ± 26	80.8 ± 3.2	1694 ± 26	0.463 ± 0.024
0.48	1.009 ± 0.022	1.024 ± 0.042	0.458 ± 0.063	1285 ± 28	86.2 ± 3.6	1827 ± 28	0.547 ± 0.030
0.52	1.011 ± 0.023	1.009 ± 0.055	0.483 ± 0.075	1338 ± 30	89.4 ± 5.4	1932 ± 35	0.607 ± 0.045
0.56	1.012 ± 0.022	0.960 ± 0.052	0.472 ± 0.063	1386 ± 30	96.3 ± 5.1	2004 ± 36	0.693 ± 0.045
0.59	0.997 ± 0.024	0.999 ± 0.043	0.452 ± 0.061	1406 ± 34	94.3 ± 4.1	2113 ± 35	0.705 ± 0.041
0.64	0.968 ± 0.028	1.000 ± 0.037	0.379 ± 0.054	1412 ± 41	96.8 ± 3.5	2192 ± 41	0.746 ± 0.040

**Figure 3.** The $f\sigma_8$ measurement from 2dFGRS (Percival et al. 2004), 6dFGS (Beutler et al. 2012), WiggleZ (Blake et al. 2011), BOSS DR12 3zbin measured using correlation function (Satpathy et al. 2017) and BOSS DR12 9zbin (our tomographic measurements). The light and dark blue shaded bands are the 68 and 95% CL prediction from Planck assuming the Λ CDM model (Planck Collaboration et al. 2016).

for 2045 mocks (see Wang et al. (2017) for details). The correlation functions are measured with a bin width of $5 h^{-1} \text{Mpc}$ on scales of $25 - 160 h^{-1} \text{Mpc}$.

3 RESULTS

3.1 Mock tests

We perform tests on the MD-Patchy mock catalogues by fitting the average of 2045 mocks. The result is shown in Table 1, where we present the mean value with 68% confidence level (CL) uncertainties of parameters α_\perp , α_\parallel and $f\sigma_8$. The fiducial cosmology we use here corresponds to the input cosmology of the mocks, therefore we expect that the average values of parameters α_\perp and α_\parallel are equal to 1. The values of $f\sigma_8$ in the fiducial cosmology are shown in the last column of Table 1. In left panels of Figure 1, we show the difference (with 68% CL uncertainty) between the mean and the expected values of parameters α_\perp , α_\parallel and $f\sigma_8$ respectively, while the panels on the right show the significance of the bias in terms of the 68% CL uncertainty. For α_\perp , the mean values are in good agreement with unity, and there is a shift of 0.005 towards higher

values in the worst case (for the last redshift bin). It is substantially smaller than the statistical uncertainty, which is 0.028. The largest bias in terms of the uncertainty is 0.18σ in the α_\perp parameter, as shown at the top right-hand panel of Figure 1. Taking this shift into account by adding the bias to the statistical error in quadrature, we find that the total uncertainty of α_\perp gets increased by 1.6%. The largest shift on the α_\parallel parameter is 0.018 towards lower values also in the last redshift bin, which is 0.37σ (the middle right-hand panel of Figure 1). This shift would increase the total uncertainty by 6.5%. The value of the $f\sigma_8$ parameter is shifted in the worst case towards higher values of 0.011, which represents 0.16σ as shown at the bottom right-hand panel of Figure 1. The shift slightly increase the total uncertainty by 1.2%. Overall, we can reproduce the input parameters in the fiducial cosmology within a shift of 0.5% for α_\perp , 1.8% for α_\parallel , and 1.1% for $f\sigma_8$ respectively.

3.2 Measurements from the data catalogue

We present the measurement from the DR12 catalogue in Table 2, showing the best-fit value with 68% CL uncertainties for parameters, α_\perp , α_\parallel and $f\sigma_8$ in each redshift slice. The one-dimensional posterior distributions and the 68 and 95% CL contour plots for these three parameters are shown in Figure 2. In the two-dimensional contour plots, we show the fiducial values of the parameters in black crosses.

Figure 3 presents our measurements of $f\sigma_8$ at different redshifts together with various other measurements, including Planck (Planck Collaboration et al. 2016), 2dFGRS (Percival et al. 2004), 6dFGS (Beutler et al. 2012), BOSS (Satpathy et al. 2017) and WiggleZ (Blake et al. 2011). To compare our measurement from the RSD measurement using the same galaxy sample in three redshift slices, as presented in Satpathy et al. (2017), we compress our measurements on $f\sigma_8$ into three redshift bins. We compress the first 4 redshift bins covering $z \in [0.2, 0.51]$ into one measurement by performing a fit as below,

$$\chi^2 = (\bar{\theta} - \theta_i) C^{-1} (\bar{\theta} - \theta_i)^T, \quad (6)$$

where, $\bar{\theta}$ is a single parameter within the redshift range of $0.2 < z < 0.51$. θ_i denote the measurements of $f\sigma_8$ in the first 4 redshift bins. C is the covariance matrix between the $f\sigma_8$ measurements in the first 4 redshift bins with other parameters marginalized over. In the same way, the measurements in the 5th and 6th z bins are compressed into one measurement and the remaining z bins are compressed into the last measurement. We find that $f\sigma_8 = 0.403 \pm 0.049$ ($0.2 < z < 0.51$); $f\sigma_8 = 0.462 \pm 0.063$ ($0.4 < z < 0.59$)

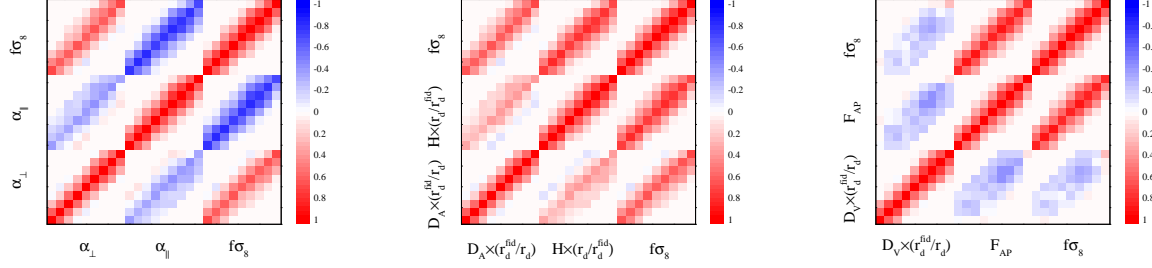


Figure 4. The correlation coefficient for the measurements, $\{\alpha_{\perp}, \alpha_{\parallel}, f\sigma_8\}$ (left panel), $\{D_A \times (r_d^{\text{fid}}/r_d), H \times (r_d/r_d^{\text{fid}})\}$ (middle panel), and $\{D_V \times (r_d^{\text{fid}}/r_d), F_{\text{AP}}\}$ (right panel) in nine redshift slices.

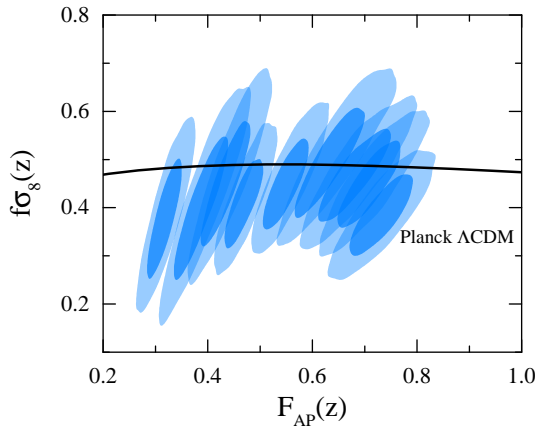


Figure 5. The 68 and 95 % CL contour plots for parameters, $f\sigma_8$ and F_{AP} in nine redshift slices. The black solid line shows the best fit model predicted from Planck in the Λ CDM framework.

and $f\sigma_8 = 0.413 \pm 0.047$ ($0.48 < z < 0.75$). These results are in agreement with that in Satpathy et al. (2017), where the measurements of correlation function multipoles were used and the GSM in theoretical framework of the Convolution Lagrangian Perturbation Theory (CLPT) (Carlson et al. 2013; Wang et al. 2014) was adopted.

As our redshift slices significantly overlap with each other, the errors of our measurements from various redshift slices are expected to correlate as well. To quantify the correlation, we perform a joint fit on parameters for all pairs of overlapping redshift bins simultaneously following Zhao et al. (2017), and calculate the correlation matrix of parameters, $\{\alpha_{\perp}, \alpha_{\parallel}, f\sigma_8\}$ in nine redshift slices. The result is shown in the left panel of Figure 4. We can see that the auto-correlation of the same parameter and the cross-correlation between different parameters decrease as the redshift separation increases. The parameter α_{\perp} anti-correlates with α_{\parallel} , and positively correlates with $f\sigma_8$. The parameters α_{\parallel} and $f\sigma_8$ negatively correlate, which is as expected.

Given α_{\perp} and α_{\parallel} , we derive the angular diameter distance, $D_A(z)r_d^{\text{fid}}/r_d$ and Hubble parameter, $H(z)r_d/r_d^{\text{fid}}$, shown in Table 2. The correlation matrix of parameters, $\{D_A r_d^{\text{fid}}/r_d, H r_d/r_d^{\text{fid}}, f\sigma_8\}$ in nine redshift slices is presented in the middle panel of Figure 4. It is seen that they positively correlate with each other, which is expected.

We present the result in another parametrization, given

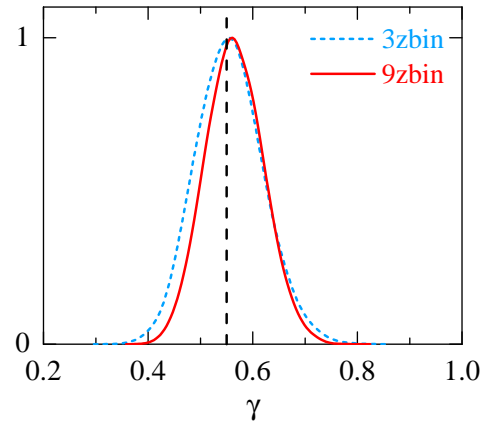


Figure 6. The one-dimensional posterior distribution of γ derived from the mock data of “3 zbins” (blue short-dashed) and “9 zbins” (red solid) respectively (see text for details). The vertical black dashed line illustrates the Λ CDM prediction as a reference.

by $\{D_V r_d^{\text{fid}}/r_d, F_{\text{AP}}, f\sigma_8\}$ where the effective volume distance $D_V(z) \equiv [cz(1+z)^2 D_A^2(z) H^{-1}(z)]^{1/3}$ and the AP parameter $F_{\text{AP}} \equiv (1+z)D_A(z)H(z)/c$, in Table 2. Their correlation matrix in nine redshift slices is shown in the right panel of Figure 4. There is a clear positive correlation between the AP parameter and $f\sigma_8$ while the parameters $D_V r_d^{\text{fid}}/r_d$ and $f\sigma_8$ are nearly uncorrelated. In the two-dimensional contour plots for parameters $f\sigma_8$ and F_{AP} , shown in Figure 5, our measurement is consistent with the Planck Λ CDM prediction within the 95% CL region for all redshift slices.

3.3 Constraints on Modified Gravity

Using our tomographic BAO and RSD measurements³, we perform an observational constraint on a phenomenological model of Modified Gravity (MG), which is parametrised by the gravitational growth index, γ , (Linder 2005; Linder & Cahn 2007) as,

$$f(a) = \Omega_m(a)^{\gamma}, \quad (7)$$

where $f(a)$ is the growth rate function of the scale factor a , and $\Omega_m(a)$ is the dimensionless matter density, i.e., $\Omega_m(a) = 8\pi G \rho_m(a)/3H^2(a)$. In the framework of General Relativity (GR),

³ The measurements and covariance matrices are available at <https://github.com/ytcosmo/TomoBAORS>

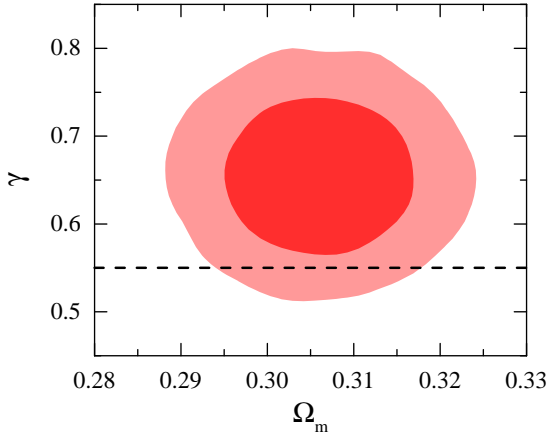


Figure 7. The 68 and 95 % CL contour plot for parameters γ and Ω_m using a combined dataset of Planck + SNe + BAO + RSD (“9 zbin”). The horizontal black dashed line illustrates the Λ CDM prediction as a reference.

the value of γ is expected to be $6/11$ (Linder 2005). Given $f(a)$, the growth factor D can be calculated via,

$$D(a) = \exp \left[- \int_a^1 da' f(a')/a' \right], \quad (8)$$

which is used to compute $\sigma_8(z)$ through

$$\sigma_8(z) = \sigma_8(z=0) \frac{D(z)}{D_{\text{GR}}(z)} \frac{D_{\text{GR}}(z_{\text{ini}})}{D(z_{\text{ini}})}. \quad (9)$$

Here we assume an initial redshift $z_{\text{ini}} = 50$, where the modification of gravity starts to take effect.

Given Eqs. (7) - (9), we can compute theoretical predictions of $f\sigma_8(z)$ at any given redshifts. We then perform an estimation of cosmological parameters with a modified version of `cosmoMC` (Lewis & Bridle 2002), sampling the following parameter space,

$$\mathbf{P} \equiv \{\omega_b, \omega_c, \Theta_s, \tau, n_s, A_s, \gamma\}, \quad (10)$$

where ω_b and ω_c are the densities of baryon and cold dark matter, Θ_s is the ratio of the sound horizon to the angular diameter distance at the decoupling epoch (multiplied by 100), τ is the optical depth, n_s and A_s are the spectral index and the amplitude of the primordial power spectrum, and γ is the growth index. We fix the sum of the neutrino mass to 0.06 eV and assume an effective number of relativistic species, $N_{\text{eff}} = 3.046$.

We use a combined data set, including the temperature and polarisation power spectra from Planck 2015 data release (Planck Collaboration et al. 2016), the “Joint Light-curve Analysis” sample of type Ia SNe (Sako et al. 2014), and a joint measurement of BAO and RSD from the BOSS DR12 completed sample in nine tomographic slices reported in this work (“9 zbins”).

Before measuring cosmological parameters including γ using the actual DR12 BAO and RSD measurement presented in Sec. 3.2, we perform a consistent test to validate our pipeline using the BAO and RSD measurement derived from the DR12 mock catalogue (see Sec. 3.1 for details of the mock catalogue). With a combined dataset of Planck + SNe + BAO (mock) + RSD (mock)⁴, we find that $\gamma = 0.565 \pm 0.054$. To quantify the information gain from the

⁴ Note that the cosmology used to generate the mock galaxy catalogue is derived from the Planck data, which is also consistent with the SNe data

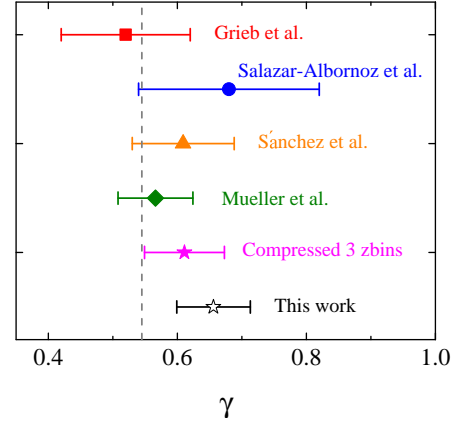


Figure 8. The constraint on the γ parameter using our measurement in comparison with those in other BOSS DR12 papers (Grieb et al. 2017; Salazar-Albornoz et al. 2017; Sánchez et al. 2017b; Mueller et al. 2016).

tomographic BAO and RSD analysis, we compress our nine-bin measurements into those at three redshift bins, and we denote the compressed measurement as “3 zbins”. We then repeat the mock test using “3 zbins” instead and find that $\gamma = 0.556 \pm 0.063$. Figure 6 compares the one-dimensional posterior distribution of γ derived from the mock data in both cases (with Planck and SNe datasets combined). As shown, both results agree well with the Λ CDM prediction of $\gamma = 0.545$ within the uncertainty, which validates our analysis, and the constraint on the precision of γ gets improved by 14%. This is because “9 zbins” is more informative in redshift, which helps with the constraint on γ as a variation of γ changes $f\sigma_8$ at different redshifts in different ways⁵.

We then apply our analysis to the actual measurement presented in Sec. 3.2, and find that $\gamma = 0.656 \pm 0.057$, which is consistent with the Λ CDM prediction within 95% CL. We show the two-dimensional contour between Ω_m and γ in Figure 7. Using the “3 zbins” measurement compressed from the actual tomographic measurement, we find $\gamma = 0.611 \pm 0.062$, which is slightly looser than that derived from our tomographic RSD measurement. The level of improvement is consistent with that using the mocks. We summarize the constraint on the γ parameter derived from other BOSS DR12 papers (Grieb et al. 2017; Salazar-Albornoz et al. 2017; Sánchez et al. 2017b; Mueller et al. 2016) in Figure 8. As shown, our measurement is in excellent agreement with these results within 68% CL, with a marginal improvement in the uncertainty.

4 CONCLUSIONS

We analyse the anisotropic clustering of the BOSS DR12 galaxies and simultaneously constrain the cosmic expansion rate and large-scale structure growth in nine overlapping redshift slices. We work

in terms of the background cosmological parameters. We removed the ISW part of the Planck data in this calculation so that neither the Planck nor SNe data are informative to infer γ .

⁵ The constraint on Ω_m also gets improved, but less significantly, namely, $\Omega_m = 0.3139 \pm 0.0071$ (3 zbins) and $\Omega_m = 0.3148 \pm 0.0070$ (9 zbins). The Figure-of-Merit (FoM) between Ω_m and γ , which is inversely proportional to the area of the 68% CL contour, is improved by 18%.

with the galaxy correlation function multipoles and adopt the GSM model to calculate the theoretical predictions. The analysis pipeline is validated using the MD-Patchy mock catalogues, before applied to the DR12 galaxy catalogue. We present the combined measurement of the effective volume distance, $D_V r_d^{\text{fid}}/r_d$, the AP parameter, F_{AP} and the parameter of linear structure growth, $f\sigma_8$. We obtain a precision of 1.5% – 2.9% for $D_V r_d^{\text{fid}}/r_d$, 5.2% – 9% for F_{AP} and 13.3% – 24% for $f\sigma_8$, depending on effective redshifts of the redshift slices. Our measurement on $f\sigma_8$ agrees with the Planck Λ CDM result within the 95% CL.

We perform a cosmological implication of our measurement (combined with Planck and SNe) to constrain γ , the gravitational growth index. We firstly validate our pipeline by reproducing the value of γ in the Λ CDM model by fitting to the BAO and RSD measurement derived from mock data. This mock test also confirms that our tomographic measurement is more informative, for the constraint on γ , than that with less redshift slices, namely, the uncertainty on γ gets tightened by 14% when “9 z bins” is used rather than “3 z bins”. We then constrain γ using our BAO and RSD measurement from the actual DR12 survey, and find that $\gamma = 0.656 \pm 0.057$, which agrees with the Λ CDM prediction within the 95% CL.

Admittedly, the information gain from the tomographic RSD measurement of BOSS DR12 is not significant, which is expected for a galaxy survey covering a moderate redshift range. However, there is much richer information on the lightcone from deeper surveys, *e.g.*, DESI⁶ and Euclid⁷, which can be extracted using our method to tighten cosmological constraints.

ACKNOWLEDGEMENTS

YW is supported by the NSFC Grant No. 11403034, and by the Young Researcher Grant of National Astronomical Observatories, Chinese Academy of Sciences. GBZ is supported by NSFC Grant No. 11673025, and by a Royal Society-Newton Advanced Fellowship. GBZ and YW are supported by National Astronomical Observatories, Chinese Academy of Sciences, and by University of Portsmouth.

Funding for SDSS-III has been provided by the Alfred P. Sloan Foundation, the Participating Institutions, the National Science Foundation, and the US Department of Energy Office of Science. The SDSS-III web site is <http://www.sdss3.org/>. SDSS-III is managed by the Astrophysical Research Consortium for the Participating Institutions of the SDSS-III Collaboration including the University of Arizona, the Brazilian Participation Group, Brookhaven National Laboratory, Carnegie Mellon University, University of Florida, the French Participation Group, the German Participation Group, Harvard University, the Instituto de Astrofísica de Canarias, the Michigan State/Notre Dame/JINA Participation Group, Johns Hopkins University, Lawrence Berkeley National Laboratory, Max Planck Institute for Astrophysics, Max Planck Institute for Extraterrestrial Physics, New Mexico State University, New York University, Ohio State University, Pennsylvania State University, University of Portsmouth, Princeton University, the Spanish Participation Group, University of Tokyo, University of Utah, Vanderbilt University, University of Virginia, University of Washington, and Yale University.

This research used resources of the National Energy Research Scientific Computing Center, which is supported by the Office of Science of the U.S. Department of Energy under Contract No. DE-AC02-05CH11231, the SCIAMO cluster supported by University of Portsmouth, and the ZEN cluster supported by NAOC.

REFERENCES

- Alam S. et al., 2015, *ApJS*, 219, 12
- Alam S. et al., 2016, *ArXiv e-prints*:1607.03155
- Alcock C., Paczynski B., 1979, *Nature*, 281, 358
- Bernardeau F., Colombi S., Gaztañaga E., Scoccimarro R., 2002, *Phys. Rep.*, 367, 1
- Beutler F. et al., 2012, *MNRAS*, 423, 3430
- Beutler F. et al., 2014, *MNRAS*, 443, 1065
- Beutler F. et al., 2017, *MNRAS*, 466, 2242
- Blake C. et al., 2011, *MNRAS*, 415, 2876
- Carlson J., Reid B., White M., 2013, *MNRAS*, 429, 1674
- Chuang C.-H. et al., 2016, *ArXiv e-prints*
- Cole S., Fisher K. B., Weinberg D. H., 1995, *MNRAS*, 275, 515
- Cole S. et al., 2005, *MNRAS*, 362, 505
- Dawson K. S. et al., 2013, *AJ*, 145, 10
- Eisenstein D., White M., 2004, *Phys. Rev. D*, 70, 103523
- Eisenstein D. J. et al., 2011, *AJ*, 142, 72
- Eisenstein D. J. et al., 2005, *ApJ*, 633, 560
- Gil-Marín H. et al., 2016, *MNRAS*, 460, 4188
- Grieb J. N. et al., 2017, *MNRAS*, 467, 2085
- Hawkins E. et al., 2003, *MNRAS*, 346, 78
- Kaiser N., 1987, *Mon. Not. Roy. Astron. Soc.*, 227, 1
- Kitaura F.-S. et al., 2016, *MNRAS*, 456, 4156
- Lewis A., Bridle S., 2002, *Phys. Rev. D*, 66, 103511
- Linder E. V., 2005, *Phys. Rev. D*, 72, 043529
- Linder E. V., Cahn R. N., 2007, *Astroparticle Physics*, 28, 481
- Matsubara T., 2008, *Phys. Rev. D*, 78, 083519
- Mehta K. T., Seo H.-J., Eckel J., Eisenstein D. J., Metchnik M., Pinto P., Xu X., 2011, *ApJ*, 734, 94
- Mueller E.-M., Percival W., Linder E., Alam S., Zhao G.-B., Sánchez A. G., Beutler F., 2016, *ArXiv e-prints*
- Okumura T., Matsubara T., Eisenstein D. J., Kayo I., Hikage C., Szalay A. S., Schneider D. P., 2008, *ApJ*, 676, 889
- Padmanabhan N., White M., 2009, *Phys. Rev. D*, 80, 063508
- Peacock J. A. et al., 2001, *Nature*, 410, 169
- Pellejero-Ibanez M. et al., 2016, *ArXiv e-prints*
- Percival W. J., White M., 2009, *MNRAS*, 393, 297
- Percival W. J., et al., 2004, *Mon. Not. Roy. Astron. Soc.*, 353, 1201
- Perlmuter S. et al., 1999, *ApJ*, 517, 565
- Planck Collaboration et al., 2016, *A&A*, 594, A13
- Raccanelli A. et al., 2013, *MNRAS*, 436, 89
- Reid B. A. et al., 2012, *MNRAS*, 426, 2719
- Reid B. A., White M., 2011, *MNRAS*, 417, 1913
- Riess A. G. et al., 1998, *AJ*, 116, 1009
- Sako M. et al., 2014, *ArXiv e-prints*:1401.3317
- Salazar-Albornoz S., et al., 2017, *Mon. Not. Roy. Astron. Soc.*, 468, 2938
- Samushia L. et al., 2013, *MNRAS*, 429, 1514
- Samushia L. et al., 2014, *MNRAS*, 439, 3504
- Sánchez A. G. et al., 2017a, *MNRAS*, 464, 1493
- Sánchez A. G. et al., 2017b, *MNRAS*, 464, 1640
- Satpathy S. et al., 2017, *MNRAS*, 469, 1369

⁶ <http://desi.lbl.gov/>

⁷ <https://www.euclid-ec.org/>

- Song Y.-S., Percival W. J., 2009, *J. Cosmology Astropart. Phys.*, 10, 004
- Vargas-Magaña M. et al., 2016, ArXiv e-prints
- Wang L., Reid B., White M., 2014, *Mon. Not. Roy. Astron. Soc.*, 437, 588
- Wang Y. et al., 2017, *MNRAS*, 469, 3762
- Zhao G.-B. et al., 2017, *MNRAS*, 466, 762